Float zone growth of Dy:$GdVO_4$ single crystals for potential use in solid-state yellow lasers

Mikio Higuchi*, Ryo Sasaki, Junichi Takahashi

Graduate School of Engineering, Hokkaido University, Sapporo 060-8628, Japan

*Corresponding author. Fax: +81-11-706-6573; E-mail: hig@eng.hokudai.ac.jp

Abstract

Single crystals of dysprosium-doped gadolinium orthovanadate (Dy:$GdVO_4$) were successfully grown by the floating zone method and their fluorescence properties were investigated. The as-grown crystals did not contain any macroscopic defects such as cracks and inclusions for any Dy-concentration of up to 4 at%. Every crystal showed optical homogeneity under the observation with a polarizing microscope; that is, no low-angle grain boundaries and growth striations were detected. In the visible region, tow distinct fluorescence bands were observed around 480 and 575 nm, corresponding to $^4F_{9/2} \rightarrow {}^6H_{15/2}$ and $^4F_{9/2} \rightarrow {}^6H_{13/2}$ transitions, respectively. The excitation spectrum for the emission of 573 nm indicates the possibility to use a commercially available laser diode of 450 nm as a pumping source for solid-state yellow laser.

PACS: 81.10.Fq

Keywords: A2. Floating zone technique; B1. Vanadates; B3. Solid sate lasers

1. Introduction

Advance in solid-state laser technology has enabled oscillations over wide wavelength regions of UV/VIS and NIR; however, there is still a blank region between 550 and 650 nm, which can not be covered even with the Ti:Al_2O_3 laser and its second harmonic. Within this region, yellow lasers of 560-590 nm have potential applications in a variety of scientific and technological fields especially in biotechnology [1,2].

Three types of systems have been developed for producing all solid-state yellow lasers, i.e., SHG of Raman laser using Nd-laser as a fundamental [3], sum-frequency mixing of Nd-laser [4] and self-frequency doubling using Yb:$YAl_3(BO_3)_4$ [5]. Two former systems are advantageous in terms of utilization of conventional Nd-lasers, but they are rather complicated and energy conversion efficiencies are relatively low. The latter also can utilize a laser diode (LD) as a pumping source, but the slope efficiency is significantly low due to the frequency conversion. Kaminskii et al. [6] reported that Dy^{3+}-doped $KGd(WO_4)_2$ and $KY(WO_4)_2$ crystals are promising for directly emitting yellow lasers, and a variety of host crystals for Dy^{3+} have subsequently been investigated [7-12]; however, a definitive host crystal for Dy^{3+} has not yet been developed.

$GdVO_4$ is known as an excellent host crystal for Nd^{3+}- and Tm^{3+}-lasers due to high absorption and emission cross sections and high thermal conductivity comparable to that of YAG. Dy-dope $GdVO_4$ single crystals have already been reported by a number of research

groups [13,14], but none of them paid attention to the fluorescence properties in the visible region. In previous studies [15-20], we have demonstrated that the floating zone method is effective to grow high-quality vanadate single crystals since no crucible is necessary and a pure oxygen flow can accordingly be used as a growth atmosphere. In fact, the float zone grown Nd:$GdVO_4$ and Tm:$GdVO_4$ single crystals exhibited high slope efficiencies [21,22].

In this study, we have successfully grown Dy:$GdVO_4$ single crystals by the floating zone method and revealed their fluorescence properties. This report proposes the possibility of Dy:$GdVO_4$ single crystals for solid-state yellow lasers with direct pumping by blue laser-diodes.

2. Experimental procedure

Powders of Gd_2O_3 (4N), V_2O_5 (4N) and Dy_2O_3 (3N) were used as starting materials. Dy-concentration was 1-4 at% in whole rare-earth elements. Feed rods for the float zone growth were prepared in the same way as described elsewhere [16].

The growth apparatus was the same image furnace as used in the previous studies [13-18]. It has double ellipsoidal mirrors with two halogen lamps of 1.5 kW as a heat source. Crystal growth was performed in the typical manner of the floating zone method. Single crystals were grown along the [110] direction at 20 mm/h with rotation rates of 5 rpm for the feed rod and 30 rpm for the seed crystal. The growth atmosphere was a pure oxygen flow of 2 liter/min.

After the post-growth annealing at 1500 °C for 10 h in air, the grown crystals were cut perpendicular and parallel to the growth direction, and then polished to be mirror finish. The polished specimens were examined with a polarizing microscope under the crossed nicol to check the optical uniformity. Wavelength dispersive electron probe microanalysis (EPMA) was performed to investigate the distribution of Dy-concentration along the growth axis. Emission and excitation spectra of the specimens cut parallel to the (001) plane were examined with a fluorescence spectrometer (JASCO-FP-6300).

3. Results and discussion

3.1. Float zone growth of Dy:$GdVO_4$

For any Dy-concentration, crack-free Dy:$GdVO_4$ single crystals were successfully grown by the floating zone method. Every as-grown crystal was transparent and colored in pale-yellow, which is intrinsic color of Dy-doped crystals due to the absorption in the blue region, indicating no coloration due to the host crystal of $GdVO_4$. Fig. 1 shows a representative Dy:$GdVO_4$ single crystal (4 at%) after the post-growth annealing. The typical dimension of the grown crystals was about 5 mm in diameter and 50 mm long.

Fig. 2 shows longitudinal and transverse cross sections of the 4 at%-doped crystal examined by polarizing microscopy with crossed nicol. No low-angle grain boundaries were present in both specimens, and growth striations could not be observed in the longitudinal section.

Furthermore, open nicol observation with a high magnification proved that this crystal contained no inclusions such as bubbles and precipitates of a second phase. These results are common for every crystal doped with different Dy-concentration, indicating that all the Dy:$GdVO_4$ single crystals grown by the floating zone method have highly optical homogeneity.

Fig. 3 shows a result on the line analysis of Dy-concentration along the growth direction measured by EPMA. The Dy-concentration was almost uniform within the measurement deviation even from the beginning of the crystal growth, which means that the effective distribution coefficient (k_{eff}) of Dy in $GdVO_4$ may be close to unity. According to Shannon [20], the ionic radii of Gd^{3+} and Dy^{3+} for 8-fold coordination are 1.053 nm and 1.027 nm, respectively. The slight difference of only 2.5 % in ionic radius is responsible to the ease with which Dy^{3+} substitutes the Gd^{3+} site. Growth striations are usually formed due to the fluctuation of impurity concentration when the difference in the ionic radius is relatively large and the k_{eff} is accordingly much lower than unity, e.g., Nd^{3+} in $Y_3Al_5O_{12}$ [24]. In the previous study [16], we have already grown striation-free Nd:$GdVO_4$ single crystals by the floating zone method. In that case, the k_{eff} of Nd^{3+} in $GdVO_4$ was estimated to be about 0.9 from the Nd-concentration profile measured by EPMA. Therefore, the striation-free Dy:$GdVO_4$ single crystals will be a natural consequence.

3.2. Fluorescence properties of Dy:$GdVO_4$

$GdVO_4$ has the tetragonal zircon-type structure; that is, $GdVO_4$ is an optically uniaxial crystal. Thus, every sample for the fluorescence measurements was cut parallel to the (001) plane in order to eliminate the polarization dependence. Fig. 4 shows a fluorescence spectrum of the 2 at%-doped Dy:$GdVO_4$ single crystal with the excitation wavelength of 300 nm. In the visible region, there are two distinct peaks of 480 nm and 575 nm bands corresponding to the transitions of $^4F_{9/2} \rightarrow {}^6H_{15/2}$ and $^4F_{9/2} \rightarrow {}^6H_{13/2}$, respectively. Since the intensity of the 575 nm band is much higher than that of the 480 nm band, only yellow luminescence can be recognized by the naked eye when the crystals was irradiated with a UV light. Although the red emission of 660 nm band ($^4F_{9/2} \rightarrow {}^6H_{11/2}$) can also be observed, its intensity is extremely lower than that of yellow emission like other Dy-doped materials [8,10,11].

Fig. 5 shows an excitation spectrum for the fluorescence of 573 nm, which is the peak wavelength of the yellow band. Above 350 nm, which corresponds to the band gap of $GdVO_4$, all the excitation peaks can be assigned to the 4f-4f transitions of Dy^{3+}. It is notable that an appreciable excitation peak is found around 450 nm, corresponding to the transition of $^6H_{15/2} \rightarrow {}^4I_{15/2}$. Excitation and emission scheme using this wavelength as a pumping source is shown in Fig. 6. Blue laser diodes (LD) of this wavelength have already been developed [25] and commercially available. Therefore, solid-state yellow lasers are expected using a Dy:$GdVO_4$ single crystal and a blue LD as a gain medium and a pumping source, respectively. If this system is realized, it will be simple and compact with high efficiency.

Every crystal with different Dy-concentration was trimmed into the same rectangular parallelepiped of about 4×4×1 mm, the square surface of which is parallel to the (001) plane, in order to examine the Dy-concentration dependence of the yellow-fluorescence intensity of Dy:$GdVO_4$. Fig. 7(a) shows yellow-fluorescence spectra with the excitation wavelength of 451 nm. All the spectra are analogous with the same peak wavelength of 573 nm as that with 300 nm excitation, independent on the Dy-concentration. The dependence of the fluorescence intensity on the Dy-concentration is shown in Fig. 7(b). There should be an optimum Dy-concentration for the yellow-fluorescence around 2 at%, above which the fluorescence intensity may be lowered because of concentration quenching.

Finally, it should be noted that blue solid-state laser may be possible using a Dy:$GdVO_4$ single crystal, even though the intensity of the blue-emission is lower than that of the yellow-emission. The fluorescence of the 480 nm band is from $^4F_{9/2}$ level to $^6H_{15/2}$ level, which is the ground state of Dy^{3+}. In such a scheme, it is usually difficult to form population inversion, which is indispensable condition for continuous laser action. However, the blue fluorescence band of Dy:$GdVO_4$ is rather wide and can be divided into five peaks with wavelengths of 474.4, 478.8, 479.5, 481.9 and 484.0 nm as shown in Fig. 8. The energy difference between the highest and lowest peaks is about 418 cm^{-1}, which is larger than thermal energy at room temperature, namely 205 cm^{-1}. Therefore, the population at the highest level of $^6H_{15/2}$ is expected to be substantially low, implying the possibility of population inversion between the lowest level of

$^4F_{9/2}$ and the highest level of $^6H_{15/2}$.

Investigation of detailed spectroscopic properties of Dy:$GdVO_4$, such as polarization dependence of absorption and emission spectra, and fluorescence lifetime, is underway, focusing on the UV/VIS regions.

4. Conclusions

Aiming for the development of solid-state yellow lasers, float zone growth of Dy:$GdVO_4$ single crystals were performed and their fluorescence properties were investigated. Every crystal was free from any macroscopic defects and had optical and compositional homogeneity. The yellow fluorescence spectrum of the 575 nm band is more intensive than the blue one of the 480 nm band, and the Dy:$GdVO_4$ crystal thus exhibited intensive yellow luminescence with the irradiation of a UV light. The fluorescence intensity reached a peak at the Dy-concentration of 2 at%. The excitation spectrum indicated that the 450 nm band is effective as a pumping source for the emission of the 575 nm band. Dy:$GdVO_4$ single crystals were found to be promising for solid-state yellow lasers using commercially available blue LDs.

References

[1] M.Bigos, N. Baumgarth, G.C. Jager, O.C. Herman, T. Nozaki, R.T. Stovel, D.R. Parks and L.A. Herzenberg, Cytometry 36 (1999) 36.

[2] W. Telford, M. Murga, T. Hawley, R. Hawley, B. Packard, A. Komoriya, F. Haas and C. Hubert, Cytometry Part A 68A (2005) 36.

[3] J. Findeisen, H.J. Eichler and A.A. Kaminskii, IEEE J. QUANTUM ELECT. 35 (1999) 173.

[4] Y.-F. Chen and S.W. Tsai, Opt. Lett. 27 (2002) 397.

[5] P.A. Burns, J.M. Dawes, P. Dekker, J.A. Piper, J. Li and J. Wang, Opt. Commun. 207 (2002) 315.

[6] A. Kaminskii, U. Hömmeric, D. Temole, J.T. Seo, K. Ueda, S. Bagayev and A. Pavlyuk, Jpn. J. Appl. Phys. 39 (2000) L208.

[7] S. Zhang, Z. Cheng, Z. Zhuo, J. Han and H. Chen, Phys. Stat. Sol. (a) 181 (2000) 485.

[8] E. Cavalli, E. Bovero and A. Belletti, J. Phys.: Condens. Matter 14 (2002) 5221.

[9] E. Cavalli, M. Bettinelli, A. Belletti and A. Speghini, J. Alloys Compd 341 (2002) 107.

[10] G. Dominiak-Dzik, P. Solarz, W. Ryba-Romanowski, E. Beregi and L. Kovács, J. Alloys Compd. 359 (2003) 51.

[11] Z. Wang, D. Yuan, X. Shi, X. Cheng, D. Xu, M.Lu and L. Pan, J. Crystal Growth 263 (2004) 246.

[12] D.K. Sardar, W.M. Bradley, R.M. Yow, J.B. Gruber and B. Zandi, J. Lumin. 106 (2004) 195.

[13] T. Shonai, M. Higuchi and K. Kodaira, Mater. Res. Bull. 35 (2000) 225.

[14] T. Shonai, M. Higuchi and K. Kodaira, J. Crystal Growth 233 (2001) 477.

[15] T. Shonai, M. Higuchi, K. Kodaira, T. Ogawa, S. Wada and H. Machida, J. Crystal Growth 241 (2002) 159-164.

[16] M. Higuchi, H. Sagae, K. Kodaira, T. Ogawa, S. Wada and H. Machida, J. Crystal Growth 264 (2004) 284.

[17] M. Higuchi, K. Kodaira, Y. Urata, S. Wada and H. Machida, J. Crystal Growth 265 (2004) 487.

[18] M. Higuchi, T. Shimizu, J. Takahashi, T. Ogawa, Y. Urata, T. Miura and S. Wada, J. Crystal Growth 283 (2005) 100.

[19] Y. Terada, T. Maeda, V. V. Kochurikhin, K. Shimamura, S. Uda and T. Fukuda. J. Crystal Growth 178 (1997) 518.

[20] H. Kimura, M. Sato, Y. Terada, K Shimamura, T. Fukuda and S. Miyashita, J. Mater. Sci. 33 (1998) 2379.

[21] T. Ogawa, Y. Urata, S. Wada, K. Onodera, H. Machida, H. Sagae, M. Higuchi and K. Kodaira, Opt. Lett. 28 (2003) 2333.

[22] R. Lisiecki, P Solarz, G. Dominiak-Dzik, W. Ryba-Romanowski, M. Sobzyk, P. Černý, J.

Šulc, H. Jeínková, Y. Urata and M. Higuchi, Phys. Rev. B 74 (2006) 035103-1.

[23] R.D. Shannon, Acta Cryst. A32 (1976) 751.

[24] R.F. Belt, R.C. Puttbach, D.A. Lepore, J. Crystal Growth 13/14 (1972) 268.

[25] S. Nakamura, M. Senoh, S. Nagahama, N. Iwasa, T. Matsushita and T. Mukai, Appl. Phys. Lett. 76 (2000) 22.

Figure captions

Fig. 1. Dy:$GdVO_4$ single crystal grown by the floating zone method (Dy-concentration: 4 at%). This crystal was annealed at 1500 °C for 10 h in air.

Fig. 2. Polarizing microphotographs of longitudinal (a) and transverse (b) cross sections of the Dy:$GdVO_4$ single crystal (Dy-concentration: 4 at%).

Fig. 3. Distribution of Dy-concentration along the growth direction (Dy-concentration: 4 at%).

Fig. 4. Fluorescence spectrum of the Dy:$GdVO_4$ single crystal (Dy-concentration: 2 at%) with the excitation wavelength of 300 nm.

Fig. 5. Excitation spectrum of the Dy:$GdVO_4$ single crystal (Dy-concentration: 2 at%) for the fluorescence wavelength of 573 nm.

Fig. 6. Excitation and emission scheme of the Dy:$GdVO_4$ using the 450 nm band as a pumping source for the yellow fluorescence of the 575 nm band.

Fig. 7. Dy-concentration dependence of the fluorescence intensity of the Dy:$GdVO_4$ single crystals with the excitation wavelength of 451 nm: (a) fluorescence spectra of 575 nm band; (b) peak intensity vs. Dy-concentration.

Fig. 8. Detailed fluorescence spectrum of the 480 nm band of the Dy:$GdVO_4$ single crystal (Dy-concentration: 2 at%).

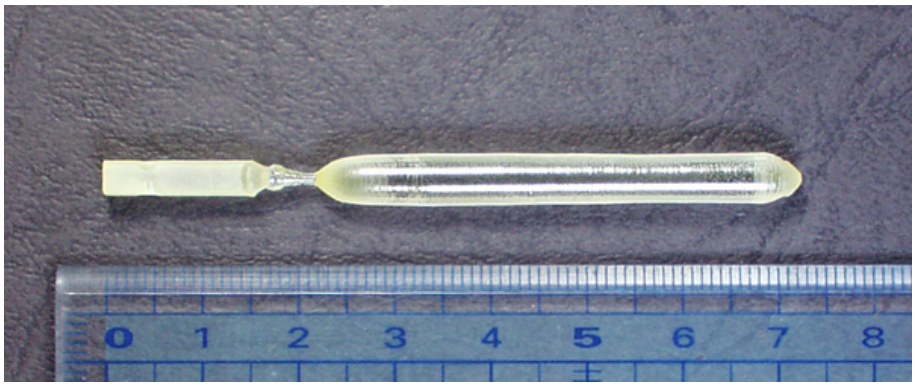

Higuchi et al., Fig. 1

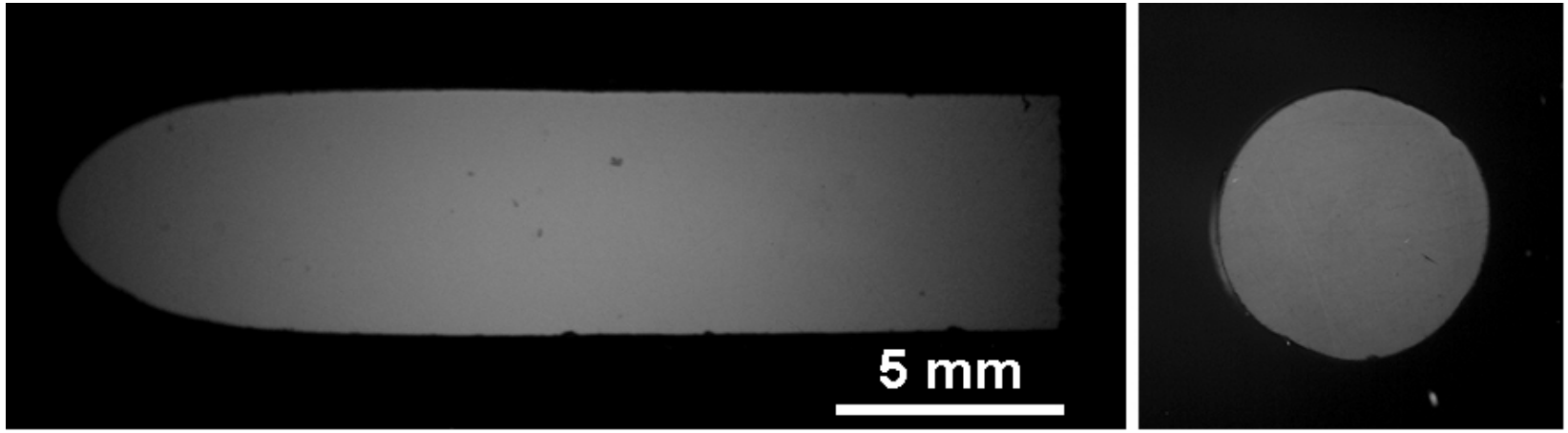

Higuchi et al., Fig. 2

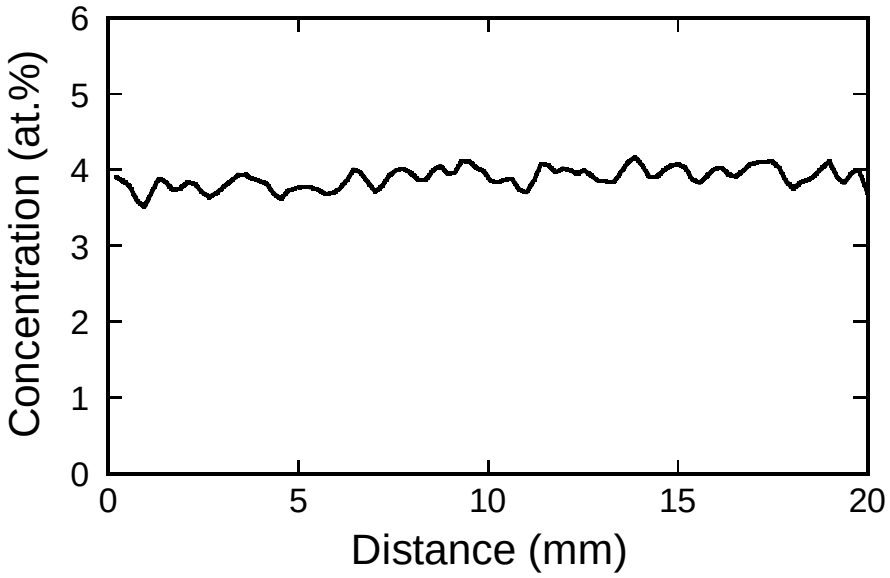

Higuchi et al., Fig. 3

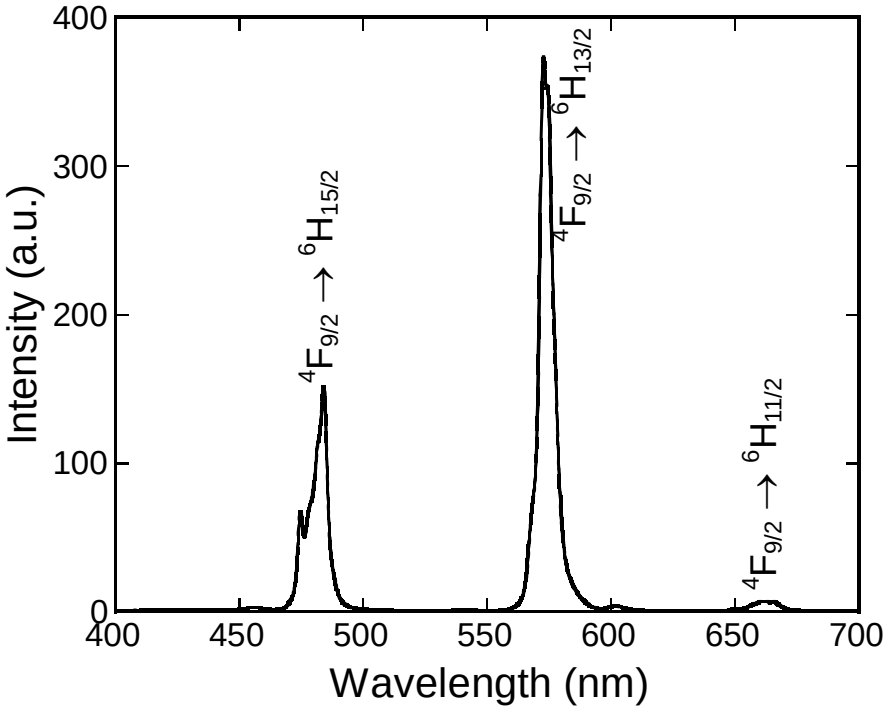

Higuchi et al., Fig. 4

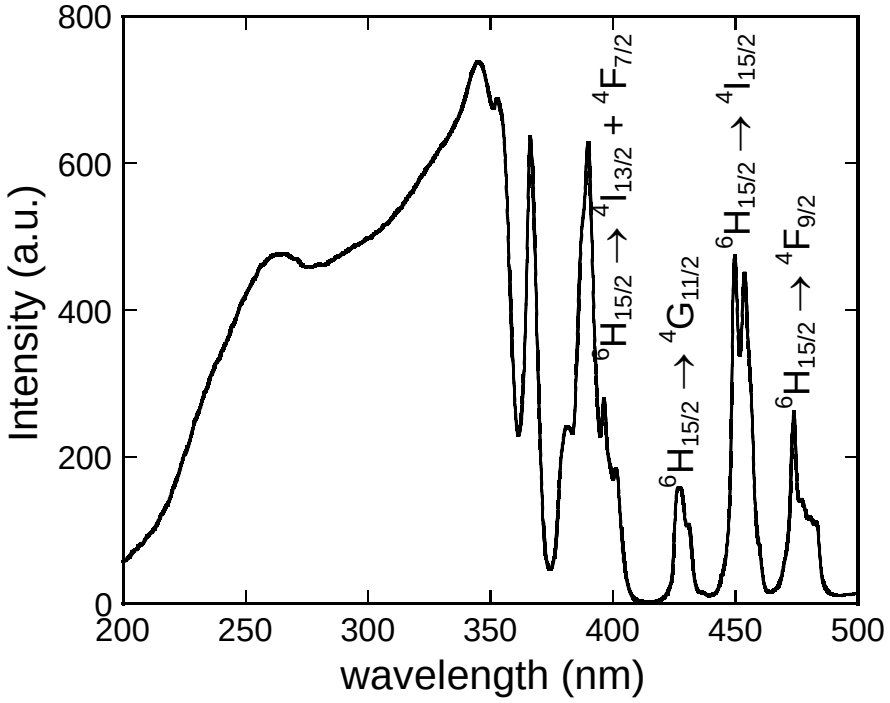

Higuchi et al., Fig. 5

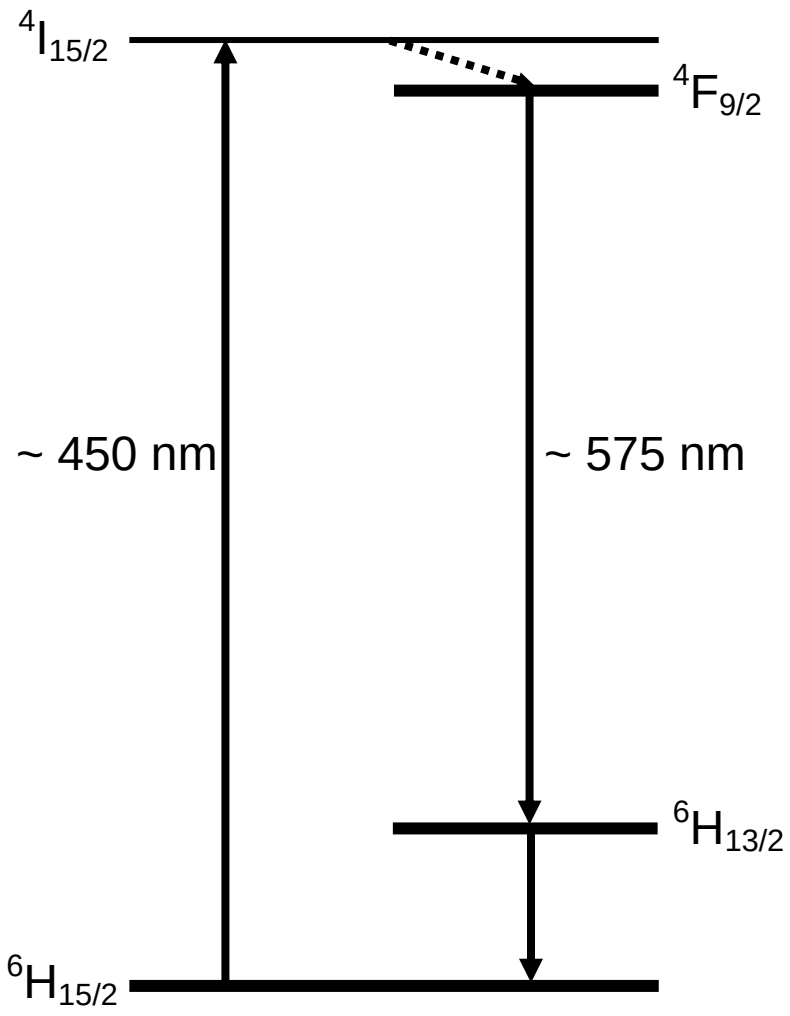

Higuchi et al., Fig. 5

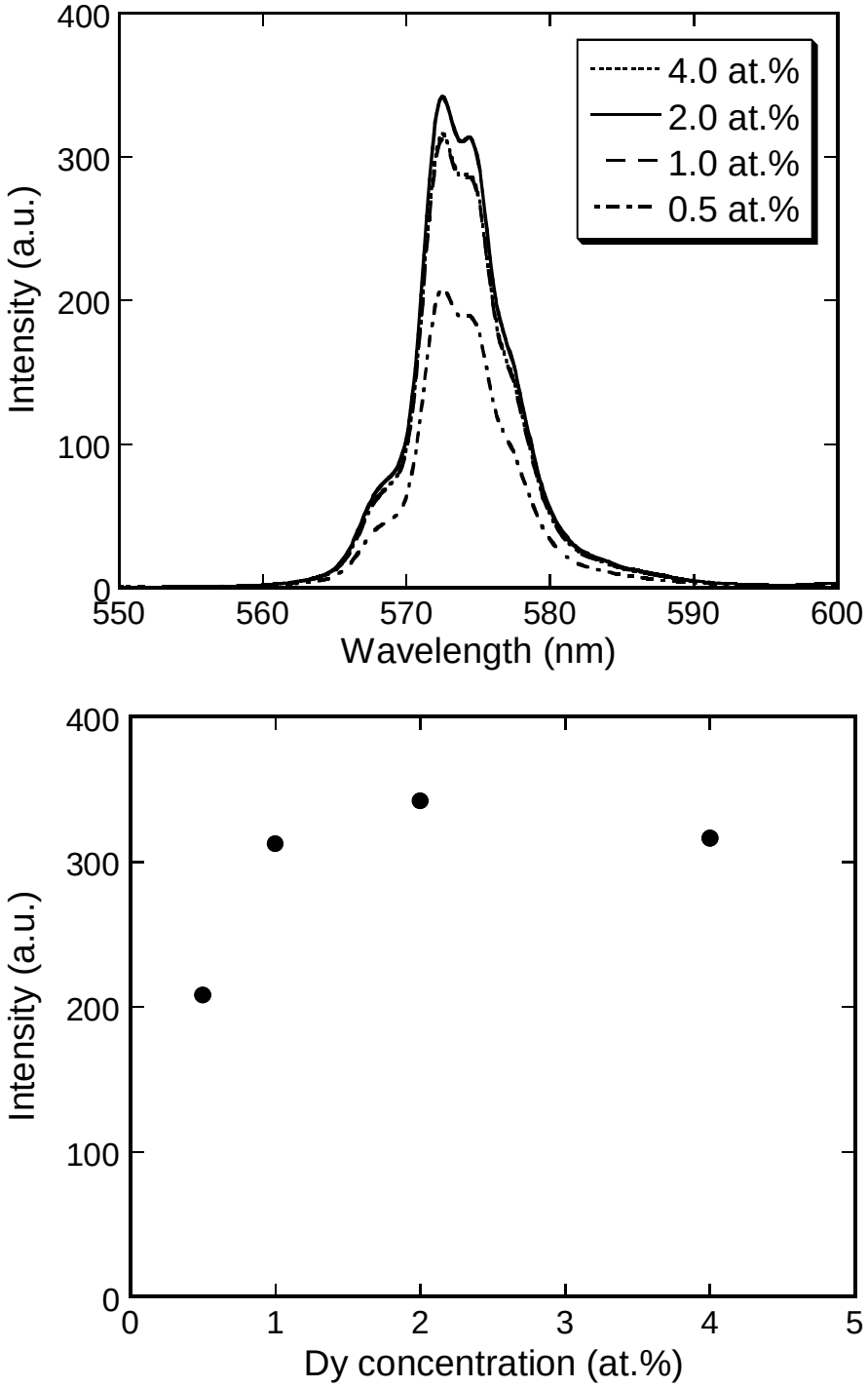

Higuchi et al., Fig. 7

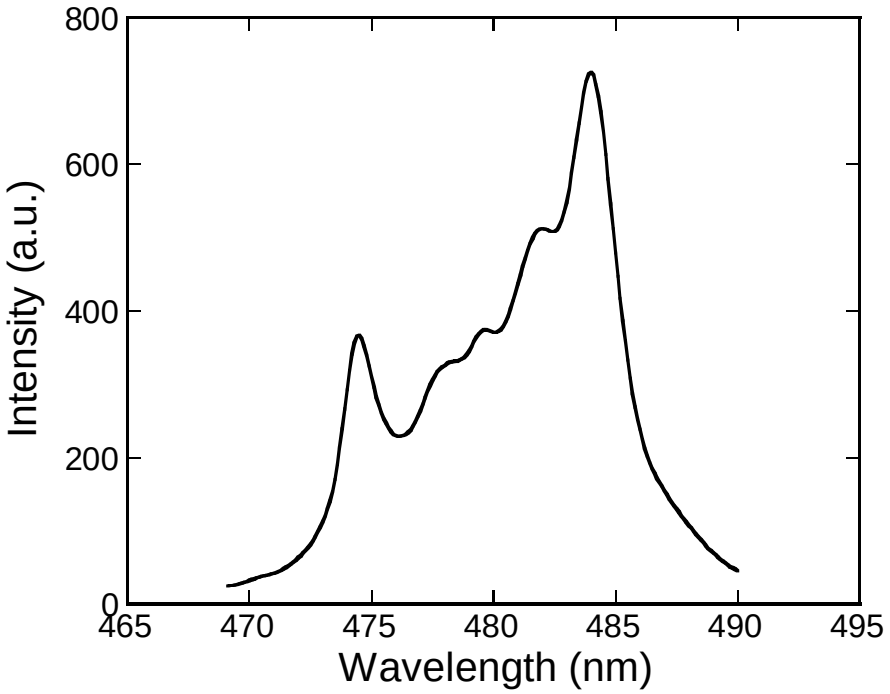

Higuchi et al., Fig. 8